

INTERNATIONAL SOCIETY FOR SOIL MECHANICS AND GEOTECHNICAL ENGINEERING



This paper was downloaded from the Online Library of the International Society for Soil Mechanics and Geotechnical Engineering (ISSMGE). The library is available here:

<https://www.issmge.org/publications/online-library>

This is an open-access database that archives thousands of papers published under the Auspices of the ISSMGE and maintained by the Innovation and Development Committee of ISSMGE.

The paper was published in the proceedings of the 20th International Conference on Soil Mechanics and Geotechnical Engineering and was edited by Mizanur Rahman and Mark Jaksa. The conference was held from May 1st to May 5th 2022 in Sydney, Australia.

Performance of geosynthetic-reinforced soil walls with marginal backfill subjected to rainfall

Performance des murs en sol renforcé géosynthétique avec remblai marginal soumis aux précipitations

Hsin-Ming Wu, Kuo-Hsin Yang & Louise Ge
Department of Civil Engineering, National Taiwan University

Ting-Ling Tseng
Trinity Foundation Engineering Consultants Co., Ltd

Benson Hsiung
Department of Civil Engineering, National Kaohsiung University of Science and Technology

ABSTRACT: Geosynthetic-reinforced soil (GRS) structures have been widely applied to numerous construction projects. Although the design guidelines recommend using coarse-grained soils as a backfill material, in-situ soil containing a high percentage of fine soils (referred to as marginal backfill) was often adopted as an alternative backfill the economic and sustainability benefits. Several case studies have reported the failure of GRS walls backfilled with in-situ fine soils under rainfall conditions. In this study, a series of model tests were performed to investigate GRS walls' performance with marginal backfill subjected to rainfall infiltration. Based on the scaling law ($N = 5$), the experimental tests model 3 m geogrid-reinforced soil walls with various reinforcement spacing $S_v = 100, 75, 60, 50$ cm in prototype subjected to rainfall with an intensity of 75 mm/hr. The distribution and variation of pore water pressures and volumetric water contents within the GRS wall model were monitored during the test. The developed wall deformation and mobilized reinforcement tensile strain were observed using digital image analysis to evaluate GRS walls' failure process and failure modes. The test results indicated the wall collapsed due to the pullout of topmost reinforcement layers for the walls with large reinforcement spacing ($S_v = 100$ and 75 cm). The use of close reinforcement spacing could effectively reduce the wall deformation and improve the wall's stability. Based on the test results, GRS walls' improved design methods against rainfall were proposed and discussed.

RÉSUMÉ: Les structures de sol géosynthétique renforcé (GRS) ont été largement appliquées à de nombreux projets de construction. Bien que les directives de conception recommandent d'utiliser des sols à gros grains comme matériau de remblai, un sol in situ contenant un pourcentage élevé de sols fins (appelé remblai marginal) a souvent été adopté comme une alternative de remblayage pour les avantages économiques et de durabilité. Plusieurs études de cas ont rapporté la rupture de murs GRS remblayés avec des sols fins in situ dans des conditions de pluie. Dans cette étude, une série de tests sur modèle a été réalisée pour étudier la performance des murs GRS avec un remblai marginal soumis à des infiltrations de pluie. Sur la base de la loi d'échelle ($N = 5$), les tests expérimentaux ont modélisé des murs de sol renforcés de géogrilles de 3 m avec différents espacements de renfort $S_v = 100, 75, 60, 50$ cm dans un prototype soumis à des précipitations d'une intensité de 75 mm / hr. La distribution et la variation des pressions interstitielles et des teneurs volumétriques en eau dans le modèle de paroi GRS ont été surveillées pendant le test. La déformation de paroi développée et la déformation de traction des armatures mobilisées ont été observées à l'aide d'une analyse d'images numériques pour évaluer les modes de rupture et de rupture des murs GRS. Les résultats des tests ont indiqué que le mur s'est effondré en raison du retrait des couches de renforcement supérieures pour les murs avec un grand espacement de renforcement ($S_v = 100$ et 75 cm). L'utilisation d'un espacement de renforcement étroit pourrait réduire efficacement la déformation du mur et améliorer la stabilité du mur. Sur la base des résultats des tests, les méthodes de conception améliorées des murs GRS contre les précipitations ont été proposées et discutées.

KEYWORDS: Geosynthetics Reinforced soil walls, Rainfall, Marginal soil, Failure mechanism.

1 INTRODUCTION

The Geosynthetic reinforced soil wall (GRS wall) is a commonly used flexible retaining structure nowadays. It has good seismic resistance and can withstand large differential settlements. It is often used in slope collapse renovation projects, road engineering, slope protection, riverbank protection. Compared with the traditional concrete structure, the structure has the advantages of economy, beauty, and environmental friendliness. However, even if the GRS wall has the above advantages, there are many excessive deformation cases or collapse due to rainfall infiltration. According to the research reports of Koerner & Koerner (2013, 2018) and Wu & Chou (2013), the leading cause of GRS walls' failure is due to heavy rainfall, insufficient compaction, and unqualified backfill, which causes it to expose to higher risks.

Due to global warming, extreme rainfall events have led to an increase in the probability of short-duration heavy rainfall events. According to the information provided by the Taiwan

Climate Change Projection and Information Platform (TCCIP), the average annual rainfall in the next 100 years increases by about 1.3 times. Both slopes and retaining structures are exposed to higher risks. To respond to global climate changes and reduce the loss of life and property, the design of retaining structures under heavy rainfall is incredibly essential. Therefore, this study discusses the failure mechanism of GRS walls under rainfall infiltration.

Backfill is one of GRS walls' main components, in which material properties directly affect the mechanical strength. Many criteria restrict the use of backfills. (Simac et al., 1993, Elias et al. 2001; AASHTO 2002; Berg et al. 2009), which are summarized in Figure 1. Generally, the fines content (pass #200) of the backfill shall not exceed 15%, and the plasticity index shall not exceed 6. If the soil particle size distribution curve does not meet the general backfill design criteria, it is called marginal soil. In engineering practice, the difficulty of obtaining, economic of consideration, and the balance of earthwork resulting in the on-site soil with higher fines content is often still used. However, the

backfill with higher fines content has lower permeability. During rainfall infiltration, as the soil saturation increases, it loses matrix suction and apparent cohesion. It is also easier to increase pore water pressure and decrease the effective stress, leading the wall to deformed or even collapse.

In addition to excessive rainfall intensity and low backfill quality, insufficient compaction is also a common problem of the GRS wall construction. Although general engineering requires compaction as high as 90% to 95%, it is still challenging to achieve in construction. For example, to avoid damage to constructing the wrap-around type retaining wall facing, other machines are used for construction and lead to insufficient compaction. Besides, construction in rainy weather makes it challenging to achieve the required degree of compaction. Therefore, in quite a lot of GRS wall failure cases, the problem of insufficient compaction does occur.

In conclusion, excessive rainfall intensity, insufficient compaction, and unqualified backfill are common problems encountered in GRS walls. Therefore, this experiment simulates the GRS wall's mechanical behavior with marginal backfill and insufficient compaction under heavy rainfall. The critical points of observation include wall deformation, shear strain, and the reinforcement's tensional strain. After a complete analysis, a design proposal for the GRS wall against rainfall is proposed.

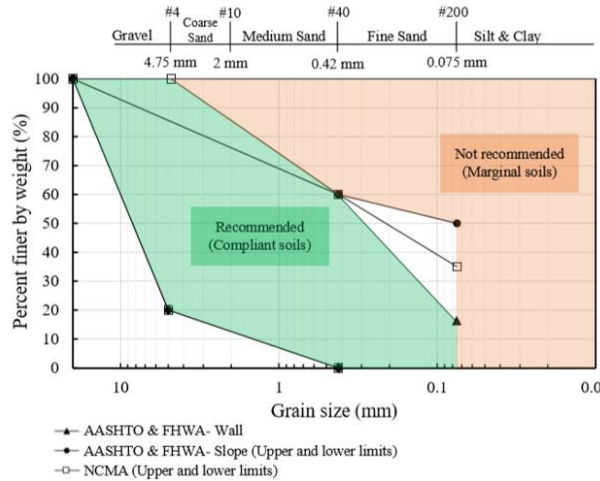


Figure 1. The particle size distribution diagram of the backfill recommended by current design codes

2 EXPERIMENTAL TEST

2.1 Material properties and scaling factors

In this research, two soils were used for the sandbox model, one for the facing filter and the other for backfill. Figure 2 shows the two soils' particle size distribution curves, and Table 1 summarizes the soil parameters. According to the Unified Soil Classification System (USCS), the former is silty sand (SM), and the latter is poorly graded sand (SP). The relevant soil tests are based on ASTM specifications are carried out. The specific gravity of the backfilled soil $G_s = 2.62$, the maximum dry unit weight, $\gamma_d = 18.1 \text{ kN/m}^3$, the water content = 10.7%, and the Relative Compaction, $R_c = 85\%$ in this study, simulating the phenomenon of slight insufficient compaction on-site, so the compacted unit weight $\gamma_d = 15.39 \text{ kN/m}^3$. According to the direct shear test, the effective friction angle after compaction = 34.6° , and the effective friction angle of saturated soil = 30.5° .

In this research, a mosquito net with an interlocking effect between particles like the geogrid was selected. A wide-width tensile test was carried out according to the recommendation of ASTM D4595 to obtain the tensile strength. As shown in Table 1, its ultimate tensile strength $T_{ult} = 1.24 \text{ kN/m}$, and its tensile stiffness $J = 7.36 \text{ kN/m}$. The interface direct shear test is also carried out according to ASTM D3080 to obtain the interface

friction coefficient between the reinforcement and the backfill. Table 1 summarizes the parameters of reinforcement.

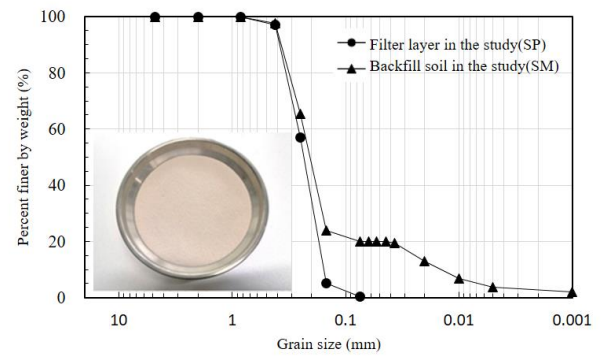


Figure 2. Soil particle size distribution curve

When conducting a reduced scale model, it is necessary to evaluate model similarity and dimensional analysis to ensure that the test results are consistent with the prototype model. As shown in Table 2, the scaling factors used in this research is $N = 5$, and the length and height of the model are 42 and 60 cm, respectively. The rainfall intensity is set to 75mm/hr to fill the instrument's limitations and the ration of permeability and rainfall intensity, which can meet the Central Meteorological Bureau's standard for extremely torrential rain. Using the relationship between rainfall intensity, duration, and frequency can be obtained in the Taipei area. The rainfall duration is 45 mins under a 100-year recurrence interval; the rainfall duration is 60 mins under a 200-year recurrence interval. According to TCCIP, in 2100, the annual rainfall accumulation is 1.3 times today and defines this as an extreme rainfall event, in which rainfall duration is set to 85 mins.

Table 1. Parameters of soil and stiffener

Properties	Value
Sand (Facing filter)	
Soil classification (USCS)	SP
Specific gravity, G_s	2.65
Mean grain size, D_{50} (mm)	0.23
Target dry unit weight, γ_d (kN/m ³)	14.9
Friction angle (as-compacted), ϕ' (°)	37.3
Hydraulic conductivity, k (m/s)	5.3×10^{-4}
Silty sand (Backfill)	
Soil classification (USCS)	SM
Specific gravity, G_s	2.62
Fines content (%)	20
Dry unit weight, γ_d (kN/m ³)	15.39
Friction angle (as-compacted), ϕ' (°)	34.6
Hydraulic conductivity, k (m/s)	5.72×10^{-6}
Reinforcement	
Type	Geogrid
Ultimate tensile strength, T_{ult} (kN/m)	1.24
Ultimate tensile strain, ϵ_{ult} (%)	16.8
Stiffness at 2% strain, J_2 (kN/m)	6
Stiffness at failure, J (kN/m)	7.36
Interface friction angle	
Silty sand-Geogrid as-compacted interface friction angle, δ (°)	29.2
Silty sand-Geogrid saturated interface friction angle, δ (°)	25.5

2.2 Model configuration

Figure 3 shows the illustration and photo of the model, in which the length, width, and height of the sandbox are 100, 30, and 90 cm, respectively, and the rainfall system is about 2 m high from the sandbox. A transparent glass plate was set in front of

the sandbox to observe the wall deformation, and a drain weep was set at the bottom of the sandbox to drain the excess rainfall to ensure that the experiment can be completed smoothly. The volumetric control method is used to compact the backfill in layers and configure the instrument at the designated position. An acrylic foundation with a length, width, and height of 85, 30,

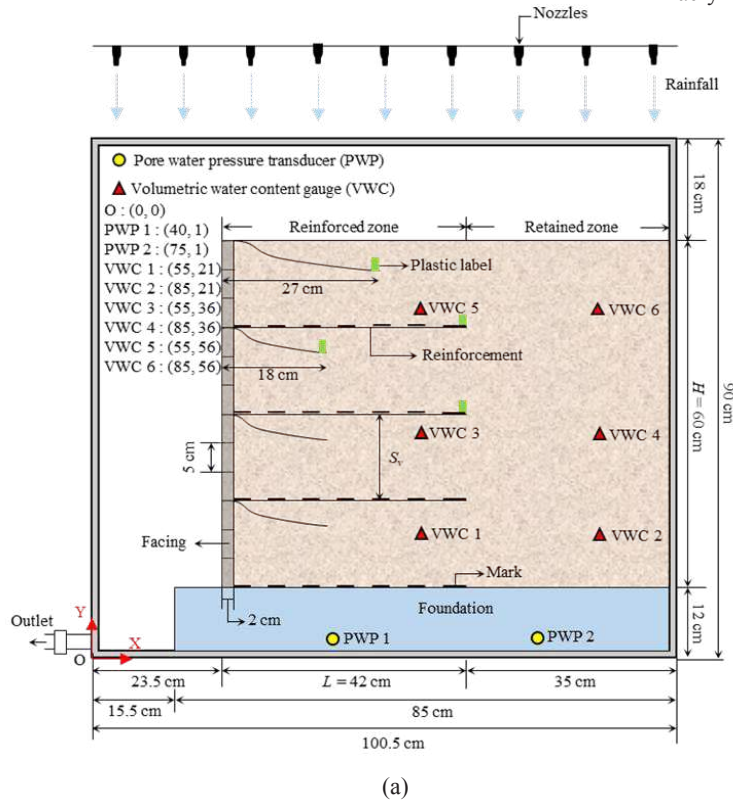


Figure 3. Test setup and sandbox: (a) illustration; (b) photo

Table 2. Scaling factors and values based on the similarity requirement

Parameters	^a Scaling factor	Model	Prototype
Geometry			
Wall height, H (m)	$1/N$	0.6	3.0
Wall length, L (m)	$1/N$	0.42	2.1
Soil parameter			
Target dry unit weight, γ_d (kN/m ³)	1	15.39	15.39
Friction angle (as-compacted), ϕ (°)	1	34.6	34.6
Hydraulic conductivity, k (m/s)	1	5.72×10^{-6}	5.72×10^{-6}
Reinforcement			
Ultimate tensile strength, T_{ult} (kN/m)	$1/N^2$	1.24	31
Stiffness at 2% strain, J_2 (kN/m)	$1/N^2$	7.36	184
Rainfall			
Intensity, I (mm/hr)	1	75	75
Duration, t (min)	$1/N$	85	425

^a Target scaling factor $N = 5$

and 12 cm was installed on the sandbox's bottom to make the

pore water pressure (PWP) gauge in a fully saturated state. The top surface of the foundation is prefabricated with several holes to ensure that the pore water pressure gauges can measure PWP accumulation. Six volumetric water content (VWC) transducers were embedded in the reinforced zone and the retained zone, respectively 9, 27, 45 cm from the retaining wall's bottom to observe water infiltration and change VWC. The reinforcement length is 0.7 times the wall height, equivalent to 42 cm, and the facing thickness is 2 cm. The overlap of the top layer reinforcement length must be lengthened to prevent the turning out failure, which is 0.6 times the length of reinforcement, and the other is 0.4 times the length of reinforcement (Balakrishnan & Viswanadham, 2019).

Table 3 summarizes the factors of safety (FS) of the internal stability analysis. In this study, the 15 cm reinforced spacing is the main case, namely SM15, where SM represents the test using silt sand, 15 represents the spacing, and the parenthesis value is the prototype size. The FS of breakage failure and pullout failure are also summarized in the table. Using as-compacted and saturated soil parameters to calculate each layer's FS and use each layer's minimum value represents the wall's FS.

3 RESULTS AND DISCUSSION

This chapter summarizes four physical test results, and converts them back to prototype for discussion, focusing on the final failure photos, digital analysis results, water infiltration and water pressure accumulation, and wall deformation at different rainfall duration. The differences between the groups are obtained through the comparison, and design suggestions are

proposed.

The rainfall intensity in this study is 75mm/hr. The following discussion uses three different rainfall durations. According to the relationship between rainfall intensity, duration, and frequency, it is obtained that in the Taipei area. Under a 100-year recurrence interval, the rainfall duration is 225 mins, and the

accumulated rainfall is 281mm, reaching the extremely heavy rain standard. Under the 200-year recurrence interval, the rainfall duration is 300 mins, and the accumulated rainfall is 375 mm, reaching the torrential rain standard, and considering the extreme

Table 3. Test program and factor of safety of the internal design

Test ID	Reinforcement spacing (cm)	Number of reinforcement layers	As-compacted		Saturated	
			FS _{breakage}	FS _{pullout}	FS _{breakage}	FS _{pullout}
SM20	20 (100)	3	3.30	3.03	2.46	1.94
SM15	15 (75)	4	3.91	3.53	2.91	2.20
SM12	12 (60)	5	4.59	4.04	3.41	2.46
SM10	10 (50)	6	5.28	4.54	3.93	2.73

Note: the values in the prototype are indicated in the parenthesis

climate of global warming, it is estimated based on TCCIP's prediction that the rainfall in the next 100 years is 1.3 times. The rainfall duration is 425 mins, and the cumulative rainfall is 531mm, reaching the standard of extremely torrential rain standard. Table 4 summarizes the results of each experiment.

3.1 Water pressure accumulative

Figure 4 shows the accumulation of water pressure for each test over time. SM 20 collapsed without water pressure accumulation because the water did not reach the bottom of the wall. SM15 collapsed at $t = 375$ mins, which accumulate 13% wall height of the water pressure. SM10 and SM12 did not collapse when the rainfall stopped, and the cumulative height of the water pressure was about 18% of the wall height.

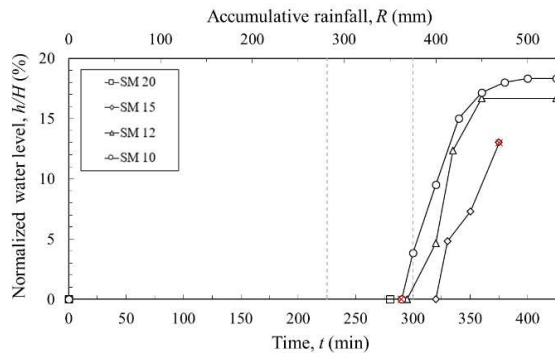


Figure 4. Comparison of the increase of phreatic level with time

3.2 Maximum deformation at the wall top

Figure 5 shows the maximum wall deformation of each test over time. The three vertical grey dotted lines in the figure are the rainfall duration of 225 mins under the 100-year interval recurrence, the rainfall duration of 300 mins under the 200-year interval recurrence, and the rainfall duration of 425 mins under extreme rainfall event. Under the condition of 100-year interval recurrence, only SM20 produces wall deformation, and the deformation exceeds 5% of the wall height. However, under the 200-year interval recurrence, SM20 has collapsed, and the deformation of the SM15 exceeds 10% of the wall height. Under extreme rainfall event, both SM20 and SM15 have collapsed. The SM12 deformation is about 5% of the wall height and tends to be stable, while SM10 has no deformation. It can be seen that reducing the reinforced spacing can delay the deformation time and reduce the deformation of the wall top.

3.3 Maximum deformation at the wall top

Figure 6 shows the final wall deformation of each test, in which the red cross represents the collapse of the wall. From the wall's deformation curve, it can be seen that SM20 is a local failure, in which a normalized height of 0-0.3 is not deformed, and the deformation at the wall top is as high as 30%H. The other test groups all belong to the overall deformation. The wall deformation generated by SM15 reached 25% and eventually collapsed. The wall deformation generated by SM12 was about 5%, while SM10 did not produce any deformation. Therefore, it can be explained that reducing the reinforced spacing can restrain the wall deformation and change the failure mode. The photos and PIV analyses of Test SM15 at various time (from the beginning of the test to the wall failure) are shown in Fig. 7.

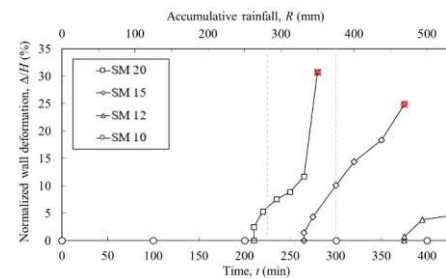


Figure 5. Comparison of the development of wall deformation with time among all tests

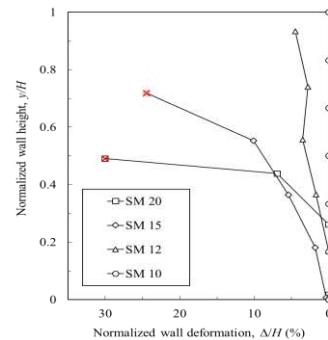


Figure 6. Comparison of the final wall deformation among all tests

Table 4. Test results

Test ID	Deformation			Time		Phreatic level	
	Δ/H at $t_{100\text{yr}}$ (%)	Δ/H at $t_{200\text{yr}}$ (%)	Δ/H at t_{extreme} (%)	Time when excessive deformation $\Delta/H > 3\%$ occurred (min)	Time when wall failure occurred (min)	Time when phreatic level rise (min)	h/H at the end of the test (%)
SM20	5.3	Collapse	Collapse	215	280	-	-
SM15	0	10.08	Collapse	270	375	320	13
SM12	0	0	4.5	380	-	295	16.7
SM10	0	0	0	-	-	290	18.7

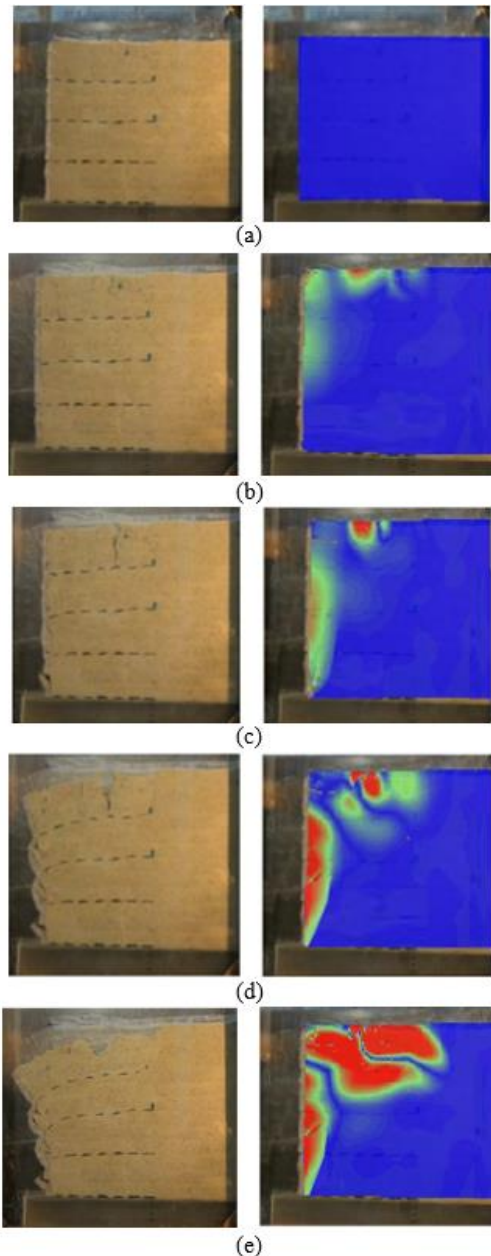


Figure 7. Photos and PIV analyses of Test SM15 at various time: $t =$ (a) 0 mins; (b) 265 mins; (c) 275 mins; (d) 325 mins; (e) 375 mins

3.4 Mobilized reinforcement tensile force

Figure 8 shows the relationship between the mobilized strain of the reinforcement in each test and the time. Since the reinforcement strain is directly related to the wall's deformation, it is evident that the test group that collapsed

before the rain stopped reach the ultimate strain at the top layer of reinforcement, for example, SM15 and SM20. However, the reinforcement strain of SM12 tends to be gentle, which means the force is not reached the ultimate state and tends to be stabilized. The SM10 does not have any deformation, so the reinforcement does not produce any deformation too.

Figure 9 shows the maximum reinforcement tensile force in each test when the rainfall stops, estimated by the reinforcement's stress-strain curve. The top of the retaining wall deforms significantly due to the rainfall, in which the maximum reinforcement tensile force in each test when the rainfall stops, estimated by the reinforcement's stress-strain curve. The top of the retaining wall deforms significantly due to the rainfall, in which the maximum tensile force occurs. It is not consistent with the traditional active earth pressure distribution, that the reason why GRS wall stability cannot be accurately estimated by active pressure.

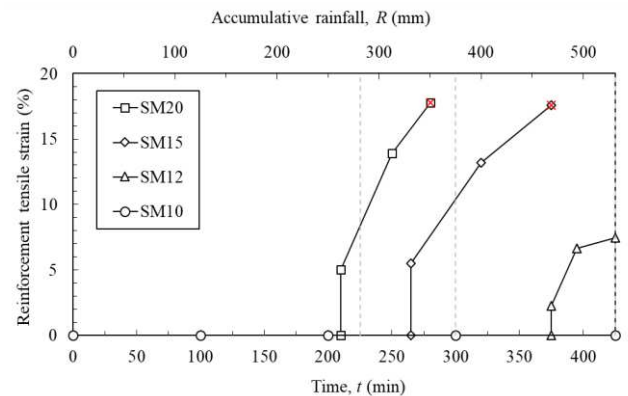


Figure 8. Comparison of the mobilized of reinforcement tensile strain with time among all tests

4 DESIGN IMPLICATION AGAINST RAINFALL

This section proposes design recommendations against rainfall based on the relationship between the FS and the wall deformation. The FS of internal stability is calculated using the saturated soil parameters in Table 3. Since there is no breakage failure observed in the test, use the pullout FS to make recommendations design subject to rainfall.

Figure 10 shows the relationship between the FS and the wall deformation time of 3% of the wall height. It can be seen from the figure that the FS and the deformation time have a high positive correlation. To ensure that the wall does not produce excessive deformation under the following conditions, if the design is carried out with a 100-year recurrence interval, the FS must be greater than 2. If designed with a 200-year recurrence interval, the FS must be greater than 2.3 in the design. If it is under extreme rainfall events, the FS must be greater than 2.7.

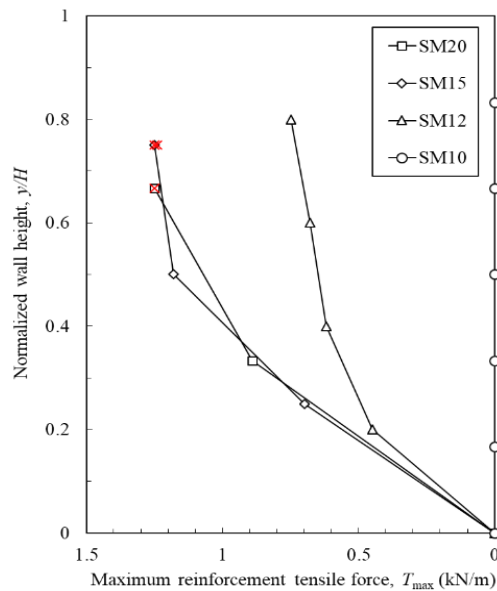


Figure 9. Comparison of the maximum reinforcement tensile force with normalized wall height among all tests

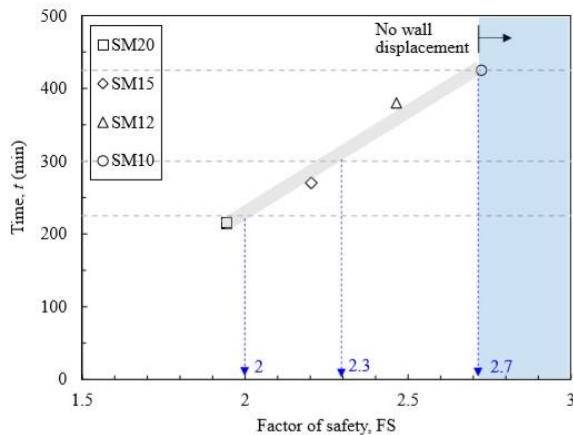


Figure 10. Relationships between the factor of safety and the time when excessive wall deformation occurred

5 CONCLUSIONS

A series of physical model tests was conducted to investigate the performance of GRS walls with different reinforcement spacing subjected to rainfall infiltration. The water infiltration time, water pressure accumulation, wall deformation, shear strain development, and failure mode were recorded in the research. Based on the above results and analysis, design suggestions under different recurrence intervals were proposed. According to the test results, the following conclusions can be concluded:

1. Reducing the reinforced spacing can delay the wall deformation and reduce the amount of deformation. When $S_v = 100$ and 75 cm in the prototype size, the GRS wall eventually collapses under the test rainfall conditions. When $S_v = 60$ cm, at the end of the test, the wall deformation is about 5% of the wall height. When $S_v = 50$ cm, the GRS wall is stable without any displacement.
2. If the reinforcement spacing is too large, such as $S_v = 100$ cm, the failure mode tends to local failure. When the spacing is reduced, the deformation tends to global failure.
3. Under rainfall intensity of 75mm/hr, in the 100-year recurrence interval design, only SM20 produces wall

deformation, and the deformation exceeds 5% of the wall height. In the 200-year recurrence interval design, SM20 has collapsed, and the deformation of the wall of SM15 exceeds 10% of the wall height. Under extreme rainfall conditions, both SM20 and SM15 have collapsed. The deformation of the SM12 is about 5% of the wall height and tends to be stable, while SM10 is no deformation.

4. Under the rainfall intensity of 75mm/hr and a rainfall duration of 425mins, this research the performance of geosynthetic-reinforced soil walls with marginal backfill subjected to rainfall. For example, under a recurrence interval of 100 years, the safety factor must be larger than 2 and should use saturated soil parameters for the calculation.

6 ACKNOWLEDGEMENTS

The financial support of this research is provided by the Ministry of Science and Technology of Taiwan under grant number MOST107- 2628-E-002-003-MY3.

7 REFERENCES

- AASHTO (2002). Standard Specifications for Highway Bridges, 17th edn. American Association of State Highway and Transportation Officials, Washington, DC, USA.
- ASTM D3080. (2011). Standard Test Method for Direct Shear Test of Soils Under Consolidated Drained Conditions", ASTM International, USA.
- ASTM D4595. (2017). "Standard Test Method for Tensile Properties of Geotextiles by the Wide-Width Strip Method ", ASTM International, USA.
- ASTM D5084. (2008). Standard Test Methods for Measurement of Hydraulic Conductivity of Saturated Porous Materials Using a Flexible Wall Permeameter. ASTM International, USA.
- ASTM D5321. (2008). Standard Test Method for Determining the Coefficient of Soil and Geosynthetic or Geosynthetic and Geosynthetic Friction by the Direct Shear Method. ASTM International, USA.
- Balakrishnan, S., and Viswanadham, B. V. S. (2019). Centrifuge model studies on the performance of soil walls reinforced with sand-cushioned geogrid layers. *Geotextiles and Geomembranes*, 47(6), 803-814.
- Berg, R., Christopher, B. R. and Samtani, N. (2009). Design of Mechanically Stabilized Earth Walls and Reinforced Soil Slopes, Report No. FHWA-NHI-10-024, vol. I and II. National Highway Institute, Federal Highway Administration, Washington, DC, USA.
- Elias, V., Christopher, B. R. and Berg, R. (2001). Mechanically Stabilized Earth Walls and Reinforced Soil Slopes Design and Construction Guidelines, Report No. FHWA-NHI-00-043. National Highway Institute, Federal Highway Administration, Washington, DC, USA.
- Koerner, R. M., and Koerner, G. R. (2013). A data base, statistics and recommendations regarding 171 failed geosynthetic reinforced mechanically stabilized earth (MSE) walls. *Geotextiles and Geomembranes*, 40, 20-27.
- Koerner, R.M., and Koerner, G.R. (2018). An extended data base and recommendations regarding 320 failed geosynthetic reinforced mechanically stabilized earth (MSE) walls. *Geotextiles and Geomembranes*, 46, 904-912.
- Simac, M., Bathurst, R. J., Berg, R. R., & Lothspeich, S. E. (1993). Design manual for segmental retaining walls (No. TR127)
- Wu, J. Y., and Chou, N. N. (2013). Forensic studies of geosynthetic reinforced structure failures. *Journal of Performance of Constructed Facilities*, 27(5), 604-613